Gut microbiome and metabolite signatures for predicting acute kidney transplant rejection: A prospective study

Hyunjeong Cho, PhD candidate,[1,2¶] Hoonsik Nam, PhD,[3¶] Hyo-Eun Kim, MS,[4] Ji Eun Kim, PhD,[5] Ji In Park, PhD,[6] Jina Park, MSc,[7] Yong Chul Kim, PhD,[8,10] Jung Pyo Lee, PhD,[9,11] Dong Ki Kim, PhD,[10,11] Kwon Wook Joo, PhD,[10,11] Yon Su Kim, PhD,[2,8,10] Bong-Soo Kim, PhD,[4] Sunghyouk Park, PhD,[3*] and Hajeong Lee, PhD,[8,10,11*]

Supplementary material

Supplemental methods

Bioinformatics analyses

The 16S rRNA gene sequencing data were processed in QIIME2 (version 2020.8)[1]. Raw paired-end FASTQ files were imported and demultiplexed using q2-demux. The demultiplexed dataset yielded a total of 11,950,707 reads across all samples, with a median of 58,457 reads per sample (mean: 54,321.4; range: 6,898–262,460).

For quality control and the generation of ASVs, we utilized the DADA2 (Divisive Amplicon Denoising Algorithm 2) plugin[2]. This process included quality filtering, denoising of reads, merging of paired-end reads, and the removal of chimeras. Based on the sequence quality plots generated from the raw data, we set the truncation length for both forward and reverse reads to 240 bp (--p-trunc-len-f 240, --p-trunc-len-r 240) to remove low-quality regions at the 3' ends. No bases were trimmed from the 5' end of the reads (--p-trim-left-f 0, --p-trim-left-r 0).

For phylogenetic analyses, the resulting representative sequences for each ASV were aligned using MAFFT[3], and a phylogenetic tree was constructed using FastTree2[4] after masking highly variable positions. The tree was then rooted at the midpoint. Taxonomic classification was assigned to the ASVs using a pre-trained Naïve Bayes classifier against the SILVA 138 (99% identity) reference database[5, 6].

Two strategies were employed to assess and mitigate contamination. First, library preparation negative controls were sequenced alongside the samples; these yielded negligible reads and were excluded, indicating no detectable reagent contamination. Second, features taxonomically classified as mitochondria or chloroplasts were filtered from the final feature table to remove potential host/environmental sequences.

To normalize for uneven sequencing depth across samples, which is crucial for diversity analyses, the ASV feature table was rarefied to a sampling depth of 1,500 reads per sample.

This depth was determined by examining the alpha rarefaction curves to ensure adequate sample coverage while maximizing sample retention.

Alpha diversity indices, reflecting observed ASVs (microbial richness) and the Shannon diversity index (microbial diversity), are presented. For β-diversity analysis, indicating differences in bacterial community composition, microbial ecology parameters were evaluated using the vegan package (v2.5-7) in R. Principal coordinates analysis (pCoA) was used to visualize distance metrics. We assessed the statistical significance of community composition comparisons using a permutational multivariate analysis of variance (PERMANOVA) test based on the Bray–Curtis dissimilarity index with 999 permutations. The effects of various clinical factors on alpha and beta diversity were evaluated, including age, sex, BMI, diabetes mellitus, desensitization, use of immunosuppressive agents, use of antibiotics and antiviral agents, induction agents, donor types, modalities, and dialysis duration.

The functions of the gut microbiome were inferred from 16S rRNA data using the phylogenetic investigation of communities by reconstruction of unobserved states (PICRUSt2) v2.3.0-b[7]. Linear discriminant analysis effect size (LEfSe) was used to determine the differentially abundant pathways between groups[8]. Pathways with a logarithmic LDA score greater than 2.5 ($P < 0.05$) were considered significantly enriched.

NMR-based stool metabolomics

Stool metabolites were extracted using deionized water obtained from a water purification system (Millipore, Rios 100, USA). Stool samples were stored at –80 °C and thawed on ice before extraction. Two hundred milligrams of aliquots were mixed in 680 μL deionized water and vortexed thoroughly. The supernatants were collected, frozen in liquid nitrogen, and thawed at 20–25 °C. After two freeze-thaw cycles, the supernatant was centrifuged at 18,500 × g for 20 min at 4 °C. Finally, 450 μL of the supernatant was mixed with 50 μL NMR buffer

(50 mM NaH_2PO_4, 20 mM Na_2HPO_4, 0.25% sodium 3-(trimethylsilyl) propionate-d4 [TSP] in deuterium oxide [D_2O]). A total of 500 μL of the mixture was loaded into a 5-mm NMR tube. Proton NMR spectra were acquired using a 600 MHz NMR spectrometer (JEOL, JNM-ECA-600, Japan) with the 1D pulse sequence "noesy-phase. ex2." The parameters included a transmitter frequency of 600.1723 MHz, spectral width of 11.261 kHz, 32,768 data points, 7 μs pulse width, 1.5 s relaxation delay, 64 scans, and a 10-minute acquisition time. The spectra were processed by phase and baseline correction and normalized to the TSP peak, referenced at 0 ppm. The processed spectra were binned to a width of 0.0358 ppm using a Perl script, numerically transformed, and subjected to univariate analysis. Spectral regions of TSP (0.0–0.4 ppm), glycerol (3.5–3.8 ppm), and water (4.2–6.0 ppm),164 bins with non-negative average areas, were selected for statistical analysis. Metabolites were identified using the Chenomx NMR Suite software (Chenomx Inc., Canada).

References

1. Bolyen, E. et al. Reproducible, interactive, scalable and extensible microbiome data science using QIIME 2. *Nat. Biotechnol.* **37**, 852-857; 10.1038/s41587-019-0209-9 (2019).

2. Callahan, B. J. et al. DADA2: high-resolution sample inference from Illumina amplicon data. *Nat. Methods* **13**, 581-583; 10.1038/nmeth.3869 (2016).

3. Katoh, K., Misawa, K., Kuma, K. & Miyata, T. MAFFT: a novel method for rapid multiple sequence alignment based on fast Fourier transform. *Nucleic Acids Res.* **30**, 3059-3066; 10.1093/nar/gkf436 (2002).

4. Price, M. N., Dehal, P. S. & Arkin, A. P. FastTree 2 - approximately maximum-likelihood trees for large alignments. *PLoS One* **5**, e9490; 10.1371/journal.pone.0009490 (2010).

5. Bokulich, N. A. et al. Optimizing taxonomic classification of marker-gene amplicon sequences with QIIME 2's q2-feature-classifier plugin. *Microbiome* **6**, 90; 10.1186/s40168-018-0470-z (2018).

6. Quast, C. et al. The SILVA ribosomal RNA gene database project: improved data processing and web-based tools. *Nucleic Acids Res.* **41**, D590-D596; 10.1093/nar/gks1219 (2013).

7. Douglas, G. M. et al. PICRUSt2: an improved and customizable approach for metagenome inference. Preprint at https://doi.org/10.1101/672295 (2020).

8. Segata, N. et al. Metagenomic biomarker discovery and explanation. *Genome Biol.* **12**, R60; 10.1186/gb-2011-12-6-r60 (2011).

Supplementary Table 1. Differentially abundant taxonomy between acute rejection and non-rejection groups

Taxonomy	wi.ep†	wi.eBH‡	rab.win.No.Rejection	rab.win.Rejection	diff.btw
d__Bacteria; p__Proteobacteria	0.02303	0.22579	5.45081	6.92957	1.63465
d__Bacteria; p__Proteobacteria; c__Gammaproteobacteria	0.02301	0.22556	5.45796	6.93123	1.60931
d__Bacteria; p__Proteobacteria; c__Gammaproteobacteria; o__Enterobacterales	0.00873	0.17724	3.61649	6.61034	2.60418
d__Bacteria; p__Proteobacteria; c__Gammaproteobacteria; o__Enterobacterales; f__Enterobacteriaceae	0.00917	0.17908	3.63918	6.56662	2.58367
d__Bacteria; p__Proteobacteria; c__Gammaproteobacteria; o__Enterobacterales; f__Enterobacteriaceae; g__Escherichia-Shigella	0.02334	0.22424	2.28383	5.22359	3.06650
d__Bacteria; p__Proteobacteria; c__Gammaproteobacteria; o__Enterobacterales; f__Enterobacteriaceae; g__Escherichia-Shigella; s__	0.02190	0.21991	2.26903	5.20889	3.18947
d__Bacteria; p__Firmicutes; c__Negativicutes	0.01015	0.18114	5.04180	3.54358	-1.33063
d__Bacteria; p__Firmicutes; c__Negativicutes; o__Acidaminococcales	0.01049	0.18003	3.92828	-0.00807	-2.12450
d__Bacteria; p__Firmicutes; c__Negativicutes; o__Acidaminococcales; f__Acidaminococcaceae	0.01052	0.17978	3.93499	0.02043	-2.22470
d__Bacteria; p__Firmicutes; c__Negativicutes; o__Acidaminococcales; f__Acidaminococcaceae; g__Phascolarctobacterium	0.00959	0.17753	3.94931	0.04171	-2.23741

†Expected p-value of Wilcoxon rank test

‡ Expected Benjamini-Hochberg corrected p-value of Wilcoxon test

rab.win.No.Rejection - median clr value for the non-rejection group

rab.win.Rejection - median clr value for the acute rejection group

diff.btw - median difference in clr values between acute rejection and non-rejection groups

Supplementary Table 2. Differentially abundant amplicon sequence variants (ASVs) between acute rejection and non-rejection groups

ASV ID*	Taxon†	wi.ep‡	wi.eBH#	rab.win.No.Rejection	rab.win.Rejection	diff.btw	Effect size
a7e39fb3e455440bb2ee624c04a2fbc4	*d__Bacteria; p__Proteobacteria; c__Gammaproteobacteria; o__Enterobacterales; f__Enterobacteriaceae; g__Escherichia-Shigella*	0.0073	0.1595	-2.6663	1.8367	3.5422	0.4252
43629854914aac4a4e21fcf1a4720365	*d__Bacteria; p__Proteobacteria; c__Gammaproteobacteria; o__Enterobacterales; f__Enterobacteriaceae; g__Escherichia-Shigella*	0.0087	0.1630	-2.9173	1.3816	3.4104	0.4192
981d989dd8301b017834b0d7fb1eb3e1	*d__Bacteria; p__Proteobacteria; c__Gammaproteobacteria; o__Enterobacterales; f__Enterobacteriaceae; g__Escherichia-Shigella*	0.0138	0.1810	-3.0925	0.2952	3.1067	0.4087
1f6a6b98aac98b1b90349278d8dd5757	*d__Bacteria; p__Proteobacteria; c__Gammaproteobacteria; o__Enterobacterales; f__Enterobacteriaceae; g__Escherichia-Shigella*	0.0273	0.2294	-2.5293	0.3146	2.7798	0.3378
9d55f42689818189ac35ea82983a73f2	*d__Bacteria; p__Proteobacteria; c__Gammaproteobacteria; o__Enterobacterales; f__Enterobacteriaceae; g__Escherichia-Shigella*	0.0398	0.2525	-2.7435	0.1843	2.8856	0.3424
eb15eff75e015db754d0222309ba2e0d	*d__Bacteria; p__Proteobacteria; c__Gammaproteobacteria; o__Enterobacterales; f__Enterobacteriaceae; g__Escherichia-Shigella*	0.0429	0.2589	-3.1480	-1.0076	2.3486	0.3020
d7129d310b09191c91788cf6a07fb839	*d__Bacteria; p__Firmicutes; c__Negativicutes; o__Acidaminococcales; f__Acidaminococcaceae; g__Phascolarctobacterium; s__Ruminococcus_sp.*	0.0454	0.2641	-0.8828	-3.3176	-2.6580	-0.3629
21213a21ccc4c236dae3dfa1c52b2d47	*d__Bacteria; p__Bacteroidota; c__Bacteroidia; o__Bacteroidales; f__Tannerellaceae; g__Parabacteroides; s__Parabacteroides_merdae*	0.0461	0.2747	0.5205	-2.0732	-1.7816	-0.2869
45797b5351fba0925db0b93937bb381c	*d__Bacteria; p__Proteobacteria; c__Gammaproteobacteria; o__Enterobacterales; f__Enterobacteriaceae; g__Escherichia-Shigella*	0.0454	0.2771	-2.0888	1.8446	2.7331	0.3126
3ed87eae740d6a80191e97cf9685ba22	*d__Bacteria; p__Proteobacteria; c__Gammaproteobacteria; o__Enterobacterales; f__Enterobacteriaceae; g__Escherichia-Shigella*	0.0473	0.2794	-2.6262	0.2874	2.5653	0.3129

* The ID of each amplicon sequence variant (ASV)
† Taxonomic information of each ASV
‡ Expected p-value of Wilcoxon rank test
# Expected Benjamini-Hochberg corrected p-value of Wilcoxon test
rab.win.No.Rejection - median clr value for the non-rejection group
rab.win.Rejection - median clr value for the acute rejection group
diff.btw - median difference in clr values between acute rejection and non-rejection groups

Supplementary Table 3. Effect of transplant period and acute rejection (AR) on the relative abundance of major taxa: Primary analysis and sensitivity analysis of the completer cohort

Dependent variable (relative abundance)	Analysis Cohort	Group (AR vs Non-AR) β (95% CI)	Time β (95% CI)	Group x Time β (95% CI)
Phascolarctobacterium	Full cohort (N=97)	**-0.0265 (-0.0488 to -0.0042)**	-0.0035 (-0.0095 to 0.0025)	0.0083 (-0.0040 to 0.0206)
	Completer cohort (N=37)	**-0.0358 (-0.0709 to -0.0007)**	-0.0032 (-0.0097 to 0.0033)	0.0109 (-0.0038 to 0.0257)
Escherichia-Shigella	Full cohort (N=97)	**0.1547 (0.0131 to 0.2963)**	**0.0546 (0.0165 to 0.0926)**	-0.0570 (-0.1350 to 0.0210)
	Completer cohort (N=37)	0.1023 (-0.1371 to 0.3417)	**0.0587 (0.0143 to 0.1032)**	-0.0405 (-0.1412 to 0.0602)

Linear mixed effects models were built in the form of Genus relative abundance ~ Group (AR vs. Non-AR) + Time (month) + Group x Time + (1|Patient). The Full cohort analysis included all available longitudinal samples from 97 patients. A sensitivity analysis was performed on the Completer cohort, which was restricted to the 37 patients who provided samples at all three time points. 95% confidence intervals (95% CI) were built using restricted maximum likelihood. 95% CI not including zero likely represents associations with $P < 0.05$. If the β coefficient for Group x Time is zero (95% CI containing 0) and the one for Group is non-zero (95% CI not containing zero), this would mean a time-independent effect by the group on genus relative abundance.

Supplementary Table 4. Baseline characteristics of the study cohort stratified by follow-up status at 12 months

	Completer (N = 37)	**Dropout** (N = 60)	***P*-value**
Demographics and anthropometrics			
Age, years	50.6 ± 10.2	49.4 ± 13.1	0.618
Male	19 (51.4)	40 (66.7)	0.198
BMI, kg/m²	22.5 ± 3.3	23.3 ± 4.0	0.301
Hospital			0.367
SMG-SNU	4 (10.8)	12 (20.0)	
SNUH	33 (89.2)	48 (80.0)	
Diabetes Mellitus	8 (21.6)	19 (31.7)	0.401
Hypertension	28 (75.7)	39 (65.0)	0.379
Cause of ESKD			0.548
Diabetes Mellitus	6 (16.2)	16 (26.7)	
Glomerulonephritis	10 (27.0)	16 (26.7)	
Hypertension	2 (5.4)	1 (1.7)	
Polycystic kidney disease	3 (8.1)	8 (13.3)	
Others	2 (5.4)	4 (6.7)	
Unknown	14 (37.8)	15 (25.0)	
Modality			0.459
Preemptive	16 (43.2)	20 (33.3)	
Hemodialysis	17 (45.9)	33 (55.0)	
Peritoneal dialysis	2 (5.4)	6 (10.0)	

Hemodialysis + Peritoneal dialysis	2 (5.4)	1 (1.7)	
Dialysis duration, months	18.6 ± 30.8	22.9 ± 35.4	0.545
Donor type			0.431
Deceased donor	8 (21.6)	8 (13.3)	
Living donor	29 (78.4)	52 (86.7)	0.616
Related	15 (40.5)	22 (36.7)	
Spouse	12 (32.4)	26 (43.3)	
Others	2 (5.4)	4 (6.7)	
ABO incompatibility	9 (24.3)	15 (25.0)	1.000
HLA mismatch			0.797
>3	17 (45.9)	30 (50.8)	
≤3	20 (54.1)	29 (49.2)	
Preformed DSA	4 (10.8)	15 (25.0)	0.148
Perioperative medication			
Antibiotics	7 (18.9)	13 (21.7)	0.947
Antiviral agent	3 (8.1)	5 (8.3)	1.000
Desensitization	12 (32.4)	19 (31.7)	1.000
IVIG + Plasmapheresis	10 (27.0)	11 (18.3)	0.450
Immunosuppressive agent	10 (27.0)	18 (30.0)	0.934
Induction agent			0.640
Anti-thymocyte globulin	4 (10.8)	9 (15.0)	
Basiliximab	33 (89.2)	49 (81.7)	
Both	0 (0.0)	1 (1.7)	
None	0 (0.0)	1 (1.7)	

Complications after KT			
Acute rejection	7 (18.9)	26 (43.3)	0.025
PTDM	12 (32.4)	5 (8.3)	0.006
Bacterial infection	8 (21.6)	16 (28.1)	0.647
Viral infection	3 (8.1)	8 (13.3)	0.646
Delayed graft function	0 (0.0)	1 (1.7)	1.000
Graft failure	1 (2.7)	2 (3.3)	1.000
Death	0 (0.0)	3 (5.0)	0.437

Values are expressed as means ± standard deviation, or n (%).

Abbreviations: BMI, body mass index; SMG-SNU, Seoul Metropolitan Government Seoul National University Boramae Medical Center; SNUH, Seoul National University Hospital; ESKD, end-stage kidney disease; HLA, human leukocyte antigen; DSA, donor-specific antibody; IVIG, intravenous immunoglobulin; KT, kidney transplantation; PTDM, posttransplant diabetes mellitus.

Supplementary Table 5. Differentially abundant taxa in rejection subtypes compared to the strict non-rejection group

Comparison Group	Taxon	Effect Size[1]	Corrected *P*-value (Welch's t-test, BH)[2]
Mixed Rejection vs. Non-Rejection	Enterobacteriaceae (unclassified genus)	-1.37	0.014
	Sutterella	-0.96	< 0.001
TCMR vs. Non-Rejection	No significant taxa identified	-	-
AMR vs. Non-Rejection	No significant taxa identified	-	-

[1]Effect Size: The median difference in centered log-ratio (clr) transformed abundances between the two groups. A negative effect size indicates enrichment in the specified rejection subtype compared to the non-rejection group.

[2]Corrected *P*-value (Welch's t-test, BH): *P*-values were calculated using Welch's t-test within the ALDEx2 framework and corrected for multiple comparisons using the Benjamini-Hochberg (BH) method. A corrected p-value < 0.05 was considered statistically significant. The non-parametric Wilcoxon rank-sum test showed a similar trend but did not reach statistical significance.

Supplementary Table 6. Differentially abundant pathway between acute rejection and non-rejection groups

BioCyc ID	MetaCyc Pathway	Superclasses	Logarithm value	Group	LDA Score	*P* value
PWY-6897	Thiamin salvage II	Cofactor, Carrier, and Vitamin Biosynthesis → Enzyme Cofactor Biosynthesis & Vitamin Biosynthesis	4.07	No rejection	2.91	0.00
HISTSYN-PWY	L-histidine biosynthesis	Amino Acid Biosynthesis	4.09	No rejection	2.89	0.00
PWY-6123	Inosine-5'-phosphate biosynthesis I	Nucleoside and Nucleotide Biosynthesis → Purine Nucleotide Biosynthesis	4.14	No rejection	2.93	0.00
PWY-6892	Thiazole biosynthesis I (E. coli)	Cofactor, Carrier, and Vitamin Biosynthesis → Enzyme Cofactor Biosynthesis & Vitamin Biosynthesis	3.90	No rejection	2.82	0.00
GLUTORN-PWY	L-ornithine biosynthesis	Amino Acid Biosynthesis	4.07	No rejection	2.90	0.00
PWY-6703	PreQ0 biosynthesis	Secondary Metabolite Biosynthesis	3.80	No rejection	2.73	0.00
PANTOSYN-PWY	Pantothenate and coenzyme A biosynthesis I	Cofactor, Carrier, and Vitamin Biosynthesis → Carrier Biosynthesis & Vitamin Biosynthesis	3.90	No rejection	2.81	0.00
PANTO-PWY	Phosphopantothenate biosynthesis I	Cofactor, Carrier, and Vitamin Biosynthesis → Carrier Biosynthesis	3.93	No rejection	2.81	0.01
PWY-6163	Chorismate biosynthesis from 3-dehydroquinate	Aromatic Compound Biosynthesis	4.10	No rejection	2.85	0.01
TRPSYN-PWY	L-tryptophan biosynthesis	Amino Acid Biosynthesis	4.01	No rejection	2.67	0.01
NONMEVIPP-PWY	Methylerythritol phosphate pathway I	Secondary Metabolite Biosynthesis	4.13	No rejection	2.93	0.01
PWY-7560	Methylerythritol phosphate pathway II	Secondary Metabolite Biosynthesis	4.13	No rejection	2.93	0.01
RIBOSYN2-PWY	Flavin biosynthesis I (bacteria and plants)	Cofactor, Carrier, and Vitamin Biosynthesis	3.95	No rejection	2.70	0.01
PWY-7219	Adenosine ribonucleotides de novo biosynthesis	Nucleoside and Nucleotide Biosynthesis	4.19	No rejection	2.92	0.01
PWY-6700	Queuosine biosynthesis	Nucleic Acid Processing	3.90	No rejection	2.69	0.01
POLYISOPRENSYN-PWY	Polyisoprenoid biosynthesis (E. coli)	Polyprenyl Biosynthesis	3.78	No rejection	2.54	0.01
PWY-5973	Cis-vaccenate biosynthesis	Fatty Acid and Lipid Biosynthesis	4.18	No rejection	2.89	0.02
PWY-6121	5-aminoimidazole ribonucleotide biosynthesis I	Nucleoside and Nucleotide Biosynthesis	4.15	No rejection	2.87	0.02
COA-PWY	Coenzyme A biosynthesis I	Cofactor, Carrier, and Vitamin Biosynthesis → Carrier Biosynthesis	4.08	No rejection	2.78	0.02
P42-PWY	Incomplete reductive TCA cycle	C1 Compound Utilization and Assimilation	3.84	No rejection	2.98	0.02
PWY-7663	Gondoate biosynthesis (anaerobic)	Fatty Acid and Lipid Biosynthesis	4.22	No rejection	2.90	0.02
PWY-6122	5-aminoimidazole ribonucleotide biosynthesis II	Nucleoside and Nucleotide Biosynthesis	4.15	No rejection	2.89	0.02
PEPTIDOGLYCANSYN-PWY	Peptidoglycan biosynthesis I (meso-diaminopimelate containing)	Cell Structure Biosynthesis	4.13	No rejection	2.84	0.02
PWY-7221	Guanosine ribonucleotides de novo biosynthesis	Nucleoside and Nucleotide Biosynthesis	4.13	No rejection	2.82	0.02
PWY-6387	UDP-N-acetylmuramoyl-pentapeptide biosynthesis I (meso-diaminopimelate containing)	Cell Structure Biosynthesis	4.13	No rejection	2.84	0.03
PWY-1269	CMP-3-deoxy-D-manno-octulosonate biosynthesis I	Carbohydrate Biosynthesis	3.80	No rejection	2.57	0.03
PWY-6385	Peptidoglycan biosynthesis III (mycobacteria)	Cell Structure Biosynthesis	4.11	No rejection	2.81	0.03
PYRIDNUCSYN-PWY	NAD biosynthesis I (from aspartate)	Cofactor, Carrier, and Vitamin Biosynthesis	3.91	No rejection	2.75	0.04
PWY-5686	UMP biosynthesis	Nucleoside and Nucleotide Biosynthesis	4.16	No rejection	2.87	0.04
PWY-6147	6-hydroxymethyl-dihydropterin diphosphate biosynthesis I	Cofactor, Carrier, and Vitamin Biosynthesis	3.90	No rejection	2.61	0.04
PWY-7315	dTDP-N-acetylthomosamine biosynthesis	Carbohydrate Biosynthesis → Sugar Biosynthesis	3.36	Rejection	2.77	0.00
PWY-5855	Ubiquinol-7 biosynthesis (prokaryotic)	Cofactor, Carrier, and Vitamin Biosynthesis → Carrier Biosynthesis	3.16	Rejection	2.71	0.00
PWY-5856	Ubiquinol-9 biosynthesis (prokaryotic)	Cofactor, Carrier, and Vitamin Biosynthesis → Carrier Biosynthesis	3.16	Rejection	2.71	0.00
PWY-5857	Ubiquinol-10 biosynthesis (prokaryotic)	Cofactor, Carrier, and Vitamin Biosynthesis → Carrier Biosynthesis	3.16	Rejection	2.71	0.00
PWY-6708	Ubiquinol-8 biosynthesis (prokaryotic)	Cofactor, Carrier, and Vitamin Biosynthesis → Carrier Biosynthesis	3.16	Rejection	2.71	0.00
ANAEROFRUCAT-PWY	Homolactic fermentation	Fermentation → Fermentation to Short-Chain Fatty Acids	3.30	Rejection	2.80	0.00
PWY-5384	Sucrose degradation IV (sucrose phosphorylase)	Carbohydrate Degradation	3.52	Rejection	2.79	0.01
PWY-6608	Guanosine nucleotides degradation III	Nucleoside and Nucleotide Degradation	3.66	Rejection	2.87	0.01
P161-PWY	Acetylene degradation	Fermentation → Fermentation of Pyruvate, or Alcohols or Short-Chain Fatty Acids	3.87	Rejection	2.72	0.01
PWY-5154	L-arginine biosynthesis III (via N-acetyl-L-citrulline)	Amino Acid Biosynthesis	3.20	Rejection	2.73	0.01
HCAMHPDEG-PWY	3-phenylpropanoate and 3-(3-hydroxyphenyl)propanoate degradation to 2-oxopent-4-enoate	Aromatic Compound Degradation	3.00	Rejection	2.59	0.01
PWY-6690	Cinnamate and 3-hydroxycinnamate degradation to 2-oxopent-4-enoate	Aromatic Compound Biosynthesis	3.00	Rejection	2.59	0.01
PWY0-1277	3-phenylpropanoate and 3-(3-hydroxyphenyl)propanoate degradation	Aromatic Compound Degradation	3.04	Rejection	2.62	0.01
COLANSYN-PWY	Colanic acid building blocks biosynthesis	Carbohydrate Biosynthesis	3.04	Rejection	2.55	0.01
PWY-6353	Purine nucleotides degradation II (aerobic)	Nucleoside and Nucleotide Degradation	3.21	Rejection	2.78	0.01
GLUCARDEG-PWY	D-glucarate degradation I	Secondary Metabolite Degradation or Carboxylate Degradation → Sugar Derivative Degradation	3.21	Rejection	2.73	0.01
GALACTARDEG-PWY	D-galactarate degradation I	Secondary Metabolite Degradation or Carboxylate Degradation→ Sugar Derivative Degradation	3.17	Rejection	2.69	0.01
PWY0-1338	Polymyxin resistance	Cell Structure Biosynthesis → Lipopolysaccharide Biosynthesis	3.05	Rejection	2.67	0.02
PENTOSE-P-PWY	Pentose phosphate pathway	Pentose Phosphate Pathways	3.66	Rejection	2.78	0.02
ECASYN-PWY	Enterobacterial common antigen biosynthesis	Carbohydrate Biosynthesis → Glycan Biosynthesis → Polysaccharide Biosynthesis	3.05	Rejection	2.66	0.02
FAO-PWY	Fatty acid β-oxidation I	Fatty Acid and Lipid Degradation	3.35	Rejection	2.95	0.02
GLUCOSE1PMETAB-PWY	Glucose and glucose-1-phosphate degradation	Carbohydrate Degradation → Sugar Degradation	3.08	Rejection	2.65	0.02
P105-PWY	TCA cycle IV (2-oxoglutarate decarboxylase)	TCA cycle	3.15	Rejection	2.72	0.02
PWY0-1296	Purine ribonucleosides degradation	Nucleoside and Nucleotide Degradation	3.79	Rejection	2.65	0.02
GLYOXYLATE-BYPASS	Glyoxylate cycle	Generation of Precursor Metabolites and Energy	3.05	Rejection	2.63	0.02
ENTBACSYN-PWY	Enterobactin biosynthesis	Secondary Metabolite Biosynthesis → Siderophore and Metallophore Biosynthesis	3.19	Rejection	2.76	0.02
P461-PWY	Hexitol fermentation to lactate, formate, ethanol and acetate	Fermentation → Fermentation of Pyruvate, or Alcohols or Short-Chain Fatty Acids	3.29	Rejection	2.76	0.02
PWY-5918	Superpathay of heme biosynthesis from glutamate	Cofactor, Carrier, and Vitamin Biosynthesis/Tetrapyrrole Biosynthesis	3.14	Rejection	2.72	0.02
HEME-BIOSYNTHESIS-II	Heme biosynthesis I (aerobic)	Cofactor, Carrier, and Vitamin Biosynthesis/Tetrapyrrole Biosynthesis	3.14	Rejection	2.72	0.02
PWY-621	Sucrose degradation III (sucrose invertase)	Carbohydrate Degradation → Sugar Degradation	3.85	Rejection	2.60	0.02
AST-PWY	L-arginine degradation II (AST pathway)	Amino Acid Degradation	3.01	Rejection	2.56	0.02
PWY0-321	Phenylacetate degradation I (aerobic)	Aromatic Compound Degradation	3.04	Rejection	2.62	0.03
P281-PWY	3-phenylpropanoate degradation	Aromatic Compound Degradation	2.96	Rejection	2.56	0.03
PWY-7446	Sulfoglycolysis	Secondary Metabolite Degradation → Sugar Derivative Degradation	2.95	Rejection	2.55	0.03
PWY-7234	Inosine-5'-phosphate biosynthesis III	Nucleoside and Nucleotide Biosynthesis → Purine Nucleotide Biosynthesis	3.31	Rejection	2.62	0.03
DAPLYSINESYN-PWY	L-lysine biosynthesis I	Amino Acid Biosynthesis	3.84	Rejection	2.52	0.03
PWY0-1261	Anhydromuropeptides recycling (peptidoglycan recycling I)	Secondary Metabolite Degradation → Sugar Derivative Degradation	3.37	Rejection	2.89	0.04
SO4ASSIM-PWY	sulfate reduction I (assimilatory)	Inorganic Nutrient Metabolism → Sulfur Compound Metabolism	3.20	Rejection	2.62	0.04
PWY-5747	2-methylcitrate cycle II	Carboxylate Degradation → Propanoate Degradation	3.01	Rejection	2.65	0.04
PPGPPMET-PWY	ppGpp biosynthesis	Metabolic Regulator Biosynthesis	3.14	Rejection	2.69	0.04
PWY0-42	2-methylcitrate cycle I	Carboxylate Degradation → Propanoate Degradation	3.01	Rejection	2.65	0.04
PWY-5837	1,4-dihydroxy-2-naphthoate biosynthesis I	Cofactor, Carrier, and Vitamin Biosynthesis → Carrier Biosynthesis	3.20	Rejection	2.70	0.04
FERMENTATION-PWY	Mixed acid fermentation	Fermentation → Fermentation of Pyruvate, or Alcohols or Short-Chain Fatty Acids	3.31	Rejection	2.86	0.04
PWY-7254	TCA cycle VII (acetate-producers)	TCA cycle	3.13	Rejection	2.66	0.04
NAD-BIOSYNTHESIS-II	NAD salvage pathway II	Cofactor, Carrier, and Vitamin Biosynthesis	3.19	Rejection	2.67	0.04
PWY0-1479	tRNA processing	Nucleic Acid Processing	3.08	Rejection	2.63	0.04
SALVADEHYPOX-PWY	Adenosine nucleotides degradation II	Nucleoside and Nucleotide Degradation	3.55	Rejection	2.95	0.04

LDA, linear discriminant analysis

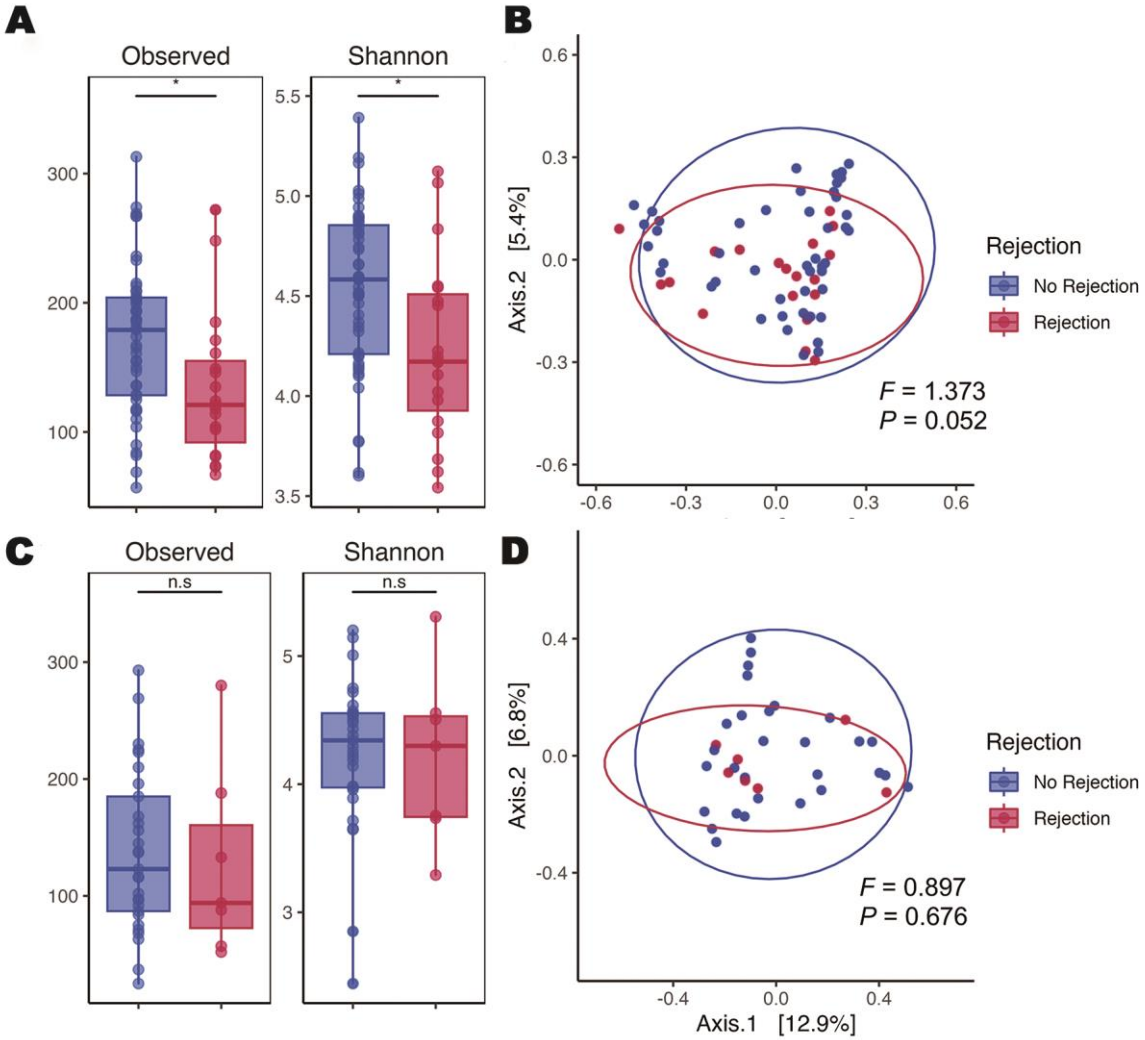

Supplementary Figure 1. Comparative analysis of gut microbial alpha and beta diversity at 3 and 12 months post-kidney transplantation. (A, B) Diversity profiles at 3 months. (A) Boxplots showing alpha diversity indices (Observed ASVs and Shannon index) comparing recipients with acute rejection (AR, red) and those without (NR, blue). (B) Principal coordinates analysis (PCoA) of Bray–Curtis distances revealed clustering patterns between groups (F = 1.373, $P = 0.052$ by PERMANOVA). (C, D) Diversity profiles at 12 months post-surgery. (C) Alpha diversity metrics indicated no significant differences between the groups (n.s.). (D) PCoA showing overlapping distributions (F = 0.897, $P = 0.676$). Each dot represents an individual. Ellipses denote the 95% confidence intervals. *$P < 0.05$; *n.s.*, not significant.

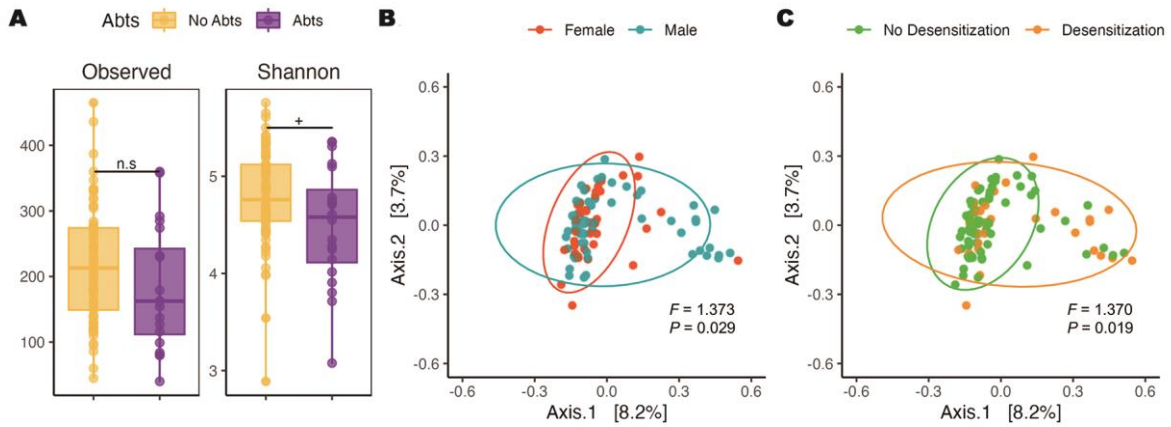

Supplementary Figure 2. Gut microbial diversity stratified by antibiotic use, sex, and desensitization status. (A) Alpha diversity comparison between pre-transplant recipients with antibiotic use (Abts, purple) and without antibiotic use (No Abts, yellow), assessed using Observed ASVs and Shannon index. A trend toward lower Shannon diversity was noted in the Abts group (+P < 0.1), and no difference was observed in richness (n.s.). (B) Beta diversity by sex using PCoA of Bray–Curtis distances shows significant clustering between female (red) and male (blue) recipients (F = 1.373, P = 0.029). (C) Beta diversity by desensitization status showed distinct separation between groups (F = 1.370, *P* = 0.019). Each dot represents a sample, and the ellipses indicate the 95% confidence intervals. *P < 0.05; +P < 0.1; n.s., not significant.*

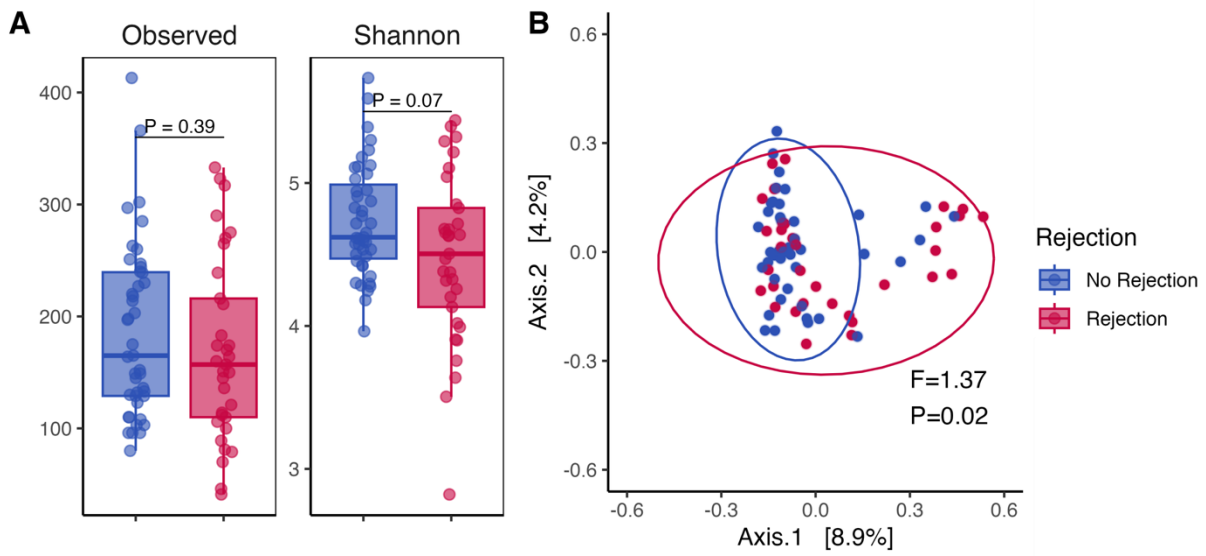

Supplementary Figure 3. Sensitivity analysis of gut microbial diversity comparing the strict non-rejection and acute rejection cohorts.

(A) Alpha diversity metrics comparing the strict non-rejection (blue; n = 43) and acute rejection (AR; red; n = 33) groups. Microbial richness (Observed ASVs, left) was not significantly different (P_{FDR} = 0.39), whereas microbial diversity (Shannon index, right) tended to be lower in the AR group (P_{FDR} = 0.07). P-values were determined using the Wilcoxon rank-sum test with Benjamini-Hochberg FDR correction. (B) Principal Coordinates Analysis (PCoA) plot based on Bray-Curtis dissimilarity, illustrating a significant difference in the overall microbial community structure between the strict non-rejection and AR groups (PERMANOVA, F = 1.37, P = 0.02). The ellipses represent the 95% confidence intervals.

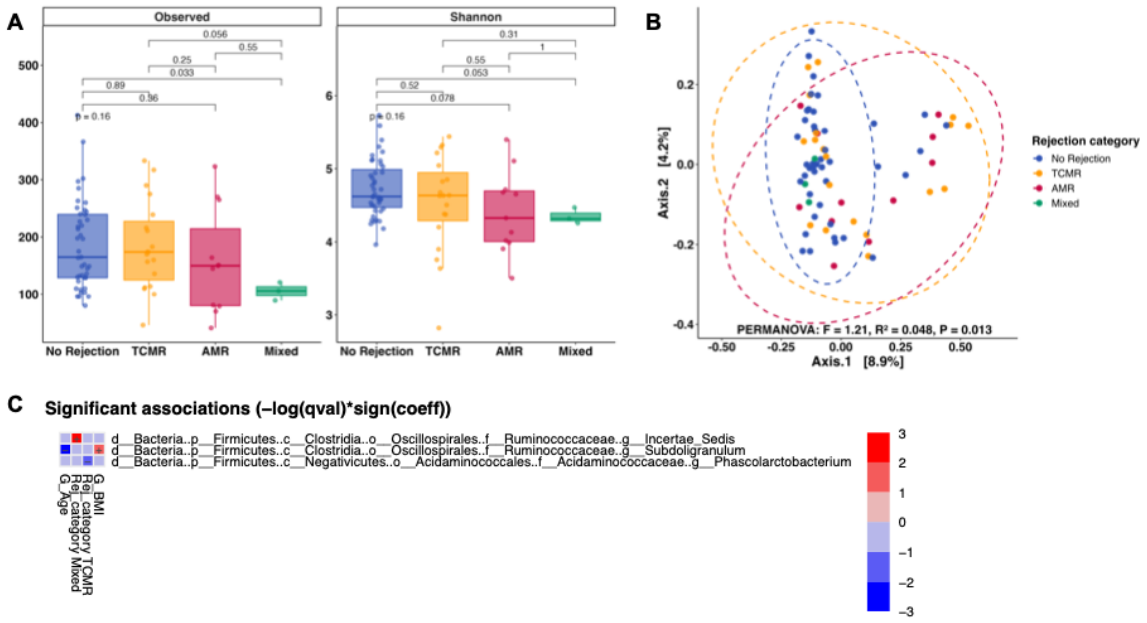

Supplementary Figure 4. Microbial diversity and taxonomic signatures of acute rejection subtypes.

(A) Alpha diversity metrics comparing the strict non-rejection cohort (n = 43) with T-cell-mediated rejection (TCMR, n = 19), antibody-mediated rejection (AMR, n = 11), and mixed rejection (n = 3) subtypes. A significant decrease in microbial richness (Observed ASVs, left) was found in the mixed rejection group compared to the non-rejection group (P_{FDR} = 0.033). A trend toward lower diversity was also observed in the AMR group for richness (P_{FDR} = 0.36) and in both the mixed and AMR groups for the Shannon index (right; P_{FDR} = 0.053 and P_{FDR} = 0.078, respectively). *P*-values were determined using the Wilcoxon rank-sum test with Benjamini-Hochberg FDR correction. (B) Principal Coordinates Analysis (PCoA) plot based on Bray-Curtis dissimilarity, illustrating a significant overall difference in microbial community structure among the four groups (PERMANOVA, F = 1.21, P = 0.013). Each point represents a sample colored by group. (C) Heatmap of significant associations from the multivariable linear model (MaAsLin) between microbial genera and rejection subtypes, adjusted for clinical covariates. The color scale represents the effect size and significance, calculated as -log(q-value) multiplied by the coefficient sign. A negative association between

Phascolarctobacterium and the TCMR subtype (coef = -0.110, q = 0.186) and a positive association between *Incertae Sedis* and the mixed rejection subtype (coef = 0.186, q = 0.115) were highlighted.